Solar Physics
DOI: 10.1007/•••••-•••-•••-••••-•

Determining the Spectral Content of MOSES Images

Jacob D. Parker[1] · **Charles C. Kankelborg**[1]

Abstract Abstract last ...

Keywords: Need to look through the list of allowed keywords and pick a couple

1. Introduction

Cite successful studies using similar data, including previous MOSES studies.

Short comings of narrow band EUV imagers. AIA temperature function for 304 Å image?. MOSES I throughput curve.

Identifying solar features in the MOSES data that have undergone spectral dispersion is simple. Subtracting the central order image (that contains no spectral dispersion) from either outboard order eliminates non-dispersed features. What remains are bi-polar features of various spatial scales. A feature in the principle wavelength, He II λ303.8Å, with a nonzero line-of-sight (LOS) velocity is translated along image rows. MOSES has a spectral dispersion of ≈ 30 km s^{-1} pixel^{-1}, leading to a less than ten pixel shift for even the fastest LOS velocities in He II. This results in a bi-polar feature with an obvious positive and negative counterpart that are immediately next to one another. A great example of this is the explosive event studied by Fox, Kankelborg, and Thomas (2010) which is highlighted in Figure **??**.

Features from other emission lines in the MOSES passband have shifts larger than 10 pixels and cannot be mistaken as Doppler shifted features in He II λ303.8 Å. A feature in Si XI λ303.3Å, the next closest line, would be shifted by 17 pixels. Si XI features can be seen on the solar limb where He II has little to no contribution. The active regions observed by MOSES have a complicated

✉ J.D. Parker
jacob.parker3@montana.edu

C.C. Kankelborg
want to include your email charles?

[1] Montana State University

structure in the difference images. The northern of the two active regions shows small bi-polar features with positive and negative lobes immediately next to one another. It also shows a large curved negative feature with no obvious positive counterpart. We will refer to this feature as the "wishbone". The wishbone has a spatial size of **find this number exactly**. Therefore its positive and negative parts should appear next to one another if it is shifted by its size or less. Since this is not the case we can infer that its wavelength is at least **so many angstroms** different. Since the wishbone's positive lobe cannot be identified by eye we turn to cross correlation to identify its spectral content.

2. Methods

2.1. Temporary Outline

I am having trouble organizing my thoughts for this section. Lets try this way.

1. Summary
2. Time Averaged Difference Images
   a) Representative Data Set (Not interested in temporal behavior)
   b) Stack Images to increase SNR.
   c) Fill in Saturated Regions
   d) Difference Images quickly reveal spectrally interesting features
3. Cross Correlation
   a) Cross Correlation Equations (Mean as a function of lag)
   b) Why Difference Images
   c) Show Cross-Correlation Function
4. Significance Testing
   a) Looking for Significant Peaks in Correlation
   b) Columns (No Spectral Dispersion)
   c) Building Longer Columns in Fourier Space
   d) Phase Shuffling for Random Data
   e) Correlation Length for Degrees of Freedom
5. Forward Model
   a) Synthetic MOSES images for different DEMs
   b) Coaligned EIT Images
   c) Chianti Temperature Image Selection and Intensity
   d) MOSES PSF Convolution
   e) Linear Combination and Least Squares Minimization with MCMC

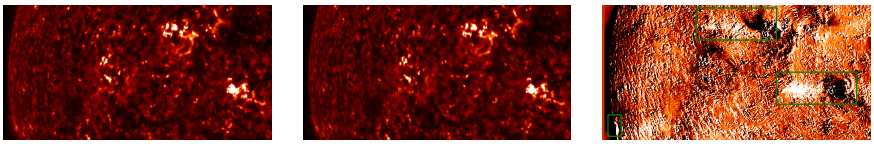

Figure 1. Figure of MOSES super exposures and a difference image

2.2. Time Averaged Difference Images

During its flight on February 8th, 2006 MOSES captured 27 images with exposure times ranging from one to thirty seconds. While MOSES did capture events with interesting temporal behavior (Fox, Kankelborg, and Thomas, 2010; Rust, 2017) our study aimed to quantify the total observed spectral content. Therefore we preformed our analysis on a time averaged version of the data.

Longer exposures are best for observing quiet sun features but are saturated near active regions. To fill in missing saturated regions and increase signal to noise we form a single time averaged image in all three spectral orders. Saturated pixels are masked with NaNs (Not a Number) and treated as missing data. Since MOSES observes through changing amounts of atmosphere throughout its flight we use the median of each image as a synthetic exposure time, rather than the amount of time the shutter is open. Masked data is then summed in time and divided by a total exposure time for each pixel to form a single time averaged image in each spectral order with no saturated pixels. Figures 1a and 1b shows the m = 0 and 1 order time averaged images.

The difference between two spectral orders reveals several interesting features. Figure 1c shows many small bipolar features throughout the quiet sun and a few large features in active regions and near the limb that are boxed in green. The northern most green box has a large, coherent, negative feature dubbed the "wishbone". The wishbone is very solar in appearance (possibly a partially filled active region loop), and has no obvious positive counterpart. Close inspection reveals a white smear to its left that is likely a shifted wishbone in the plus order. Unfortunately the positive portion of the wishbone is too blurry to quantify its shift by inspection. In order to quantify subtle differences between orders we turn to cross-correlation.

2.3. Cross-Correlation

To help identify subtle pattern repetition in the MOSES difference images we cross-correlated them along the dispersion direction, or image rows. The cross-correlation of two difference images is defined to be,

$$PZ \otimes MZ = \mathcal{F}^{-1}\left\{\mathcal{F}\left(PZ\right) * \mathcal{F}\left(MZ\right)\right\}, \tag{1}$$

where PZ and MZ are the m = 0 order subtracted from the m = 1 order and the m = 0 order subtracted from the m = -1 order respectively. $\mathcal{F}$ is the Fast

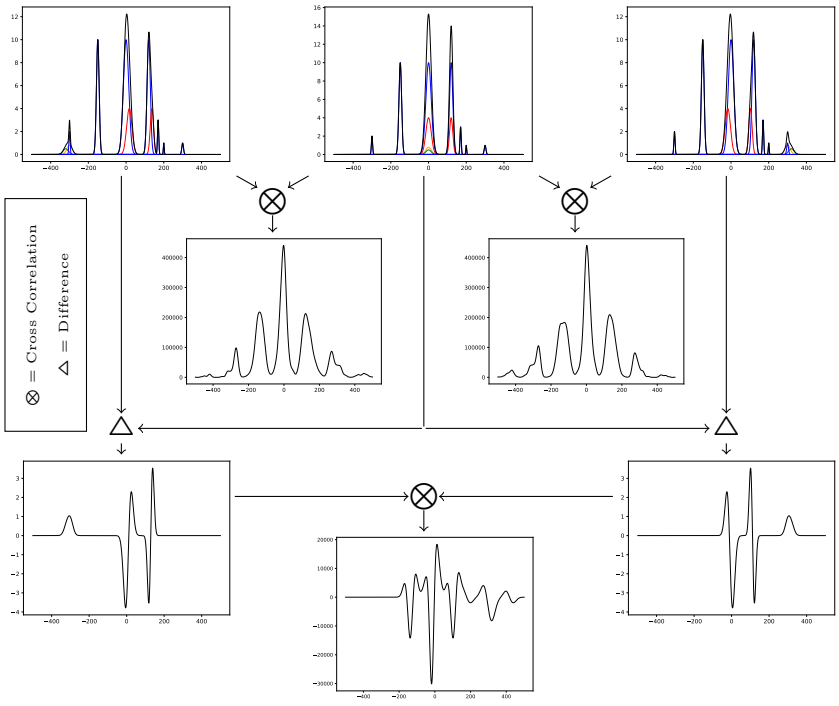

Figure 2. A graphical representation of our cross-correlation procedure

Fourier Transform (FFT) operator. The MOSES image rows were also Hanning windowed prior to applying the FFT to minimize edge effects. The discrete Hanning window, $w(k)$, implemented was,

$$w(k) = \alpha - (1-\alpha)\cos\left(\frac{2\pi k}{N}\right) \text{ for } k = 0, 1, ..., N-1 \quad , \tag{2}$$

where N is the number of elements in the array being windowed and $\alpha = .5$.

Preforming a cross-correlation on the difference images requires justification. An obvious first choice would have been to simply cross-correlate the m = 0 order with either outboard order. Unfortunately the correlation function is dominated by the autocorrelation of the He II signal as seen in Figure 2(put a letter here). This would also be the case when cross-correlating the m = 1 and m = -1 order images. By taking the difference we remove stationary He II objects from the images and in turn their autocorrelation from the cross-correlation functions.

This procedure yields a one dimensional cross-correlation function for each row of the MOSES difference images. Since we are concerned mostly with bulk spectral content we then take the mean of all 1024 cross-correlation functions, one for each row, to get our final correlation curve plotted in blue in Figure 3.

The cross-correlation curve or the MOSES difference images has a few notable features. There are several noticeable peaks in correlation at approximately

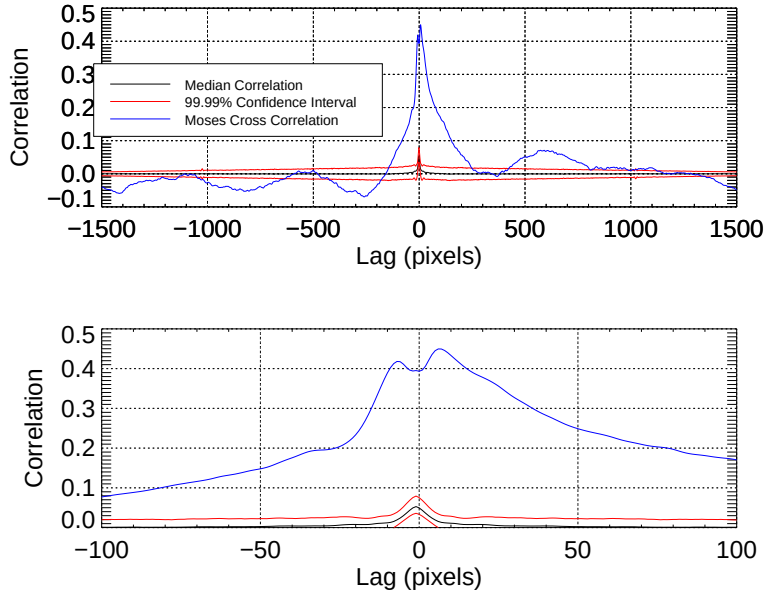

Figure 3. The mean cross-correlation function of MOSES difference image rows (blue) overlaid on the 99.99 percent confidence interval formed by cross-correlating random data (red).

−800, 250, and 600 pixel lags. The largest peak in correlation, centered about zero lag, also displays a double peak, not typical of auto-correlation functions that generally have maxima at zero lag for uncorrelated functions. While these features are identifiable, the curve is complicated enough that quantifying peaks in correlation visually is difficult and the significance of any given peak is questionable. We therefore move to test the null hypothesis that none of these features are statistically significant by cross-correlating random data generated to match the MOSES image rows.

2.4. Significance Testing

The mean cross-correlation function of the two MOSES difference images, PZ and MZ, has several peaks at nonzero lags. We propose that these peaks in cross-correlation are due to shifted solar features in the MOSES outboard orders and are therefore significant in identifying extra spectral content. To test this hypothesis we cross correlated randomly generated synthetic solar data that matched MOSES image rows in length and had similar power spectral and autocorrelation distributions. Our test data set was generated from the MOSES image columns because they contain the same solar features as the image rows, but contain practically no spectral dispersion. By interpolating and shuffling

the elements of the MOSES columns in Fourier space we can generate a large number of test arrays for significance testing.

MOSES images contain 2048 columns. These columns have the same spatial features as MOSES image rows but with none of the spectral information. Despite this the MOSES image columns are insufficient for significance testing in a couple ways. First, there is an insufficient sample size. With features in the MOSES images ranging from four to about a hundred pixels we have at most 512 unique columns for significance testing. Second, they are half as long as the rows preventing us from measuring significance past 1024 pixel lag. Therefore we needed to generate a synthetic data set for significance testing.

Using the MOSES image columns as our basis we generated N random arrays that are 2048 long and match MOSES columns in both power spectral and autocorrelation distribution. First the columns in each image, $P(x,y)$, $Z(x,y)$, and $M(x,y)$, are windowed with a Hanning window, $w(y)$(Equation 2), and Fourier transformed along the column dimension, y. The windowed Fourier transformed array is defined to be

$$\widetilde{Z}_w[x,k] = \mathcal{F}_y\left[w(y)Z[x,y]\right], \tag{3}$$

where, $x = 0, 1, ..., 2047$ and $y = 0, 1, ..., 1023$. In Equation 3 and the following equations we will show the procedure used to generate random arrays for only the zero order, $Z(x,y)$, for simplicity even though an identical procedure was carried out on every order.

The transformation outlined in Equation 3 gives us 511 spatial frequency bins and one DC bin that each have 1024 elements, one for each column, for each order. Each new array, $\widetilde{Z}'$, is formed by picking an element randomly from each frequency bin. To further scramble the array each value of k, aside from the DC term, is given a random phase shift, $e^{i\phi}$. By this method the k^{th} element in each new synthetic array, $\widetilde{Z}'_k$, is found as follows:

$$\widetilde{Z}'_k = \widetilde{Z}_w\left[\sigma(m, 2048), k\right] e^{i\Phi(n)}, \tag{4}$$

where,

$$\sigma(m, L) = floor\{randomu(m) * L\}, \tag{5}$$

$$\Phi(n) = 2\pi * randomu(n), \tag{6}$$

the function $randomu()$ picks a random value from a uniform distribution between zero and one each time it is called, and $floor()$ rounds down to the nearest integer. The function $\sigma()$ generates an random integer between zero and $L-1$.

In order create an array that is 2048 elements long from one that is 1024 elements long we require twice as many value of k. We solve this problem by double picking values from the distribution for each wave number, k. The values of k used in Equation 4 are

$$k_j = floor(j/2), \tag{7}$$

for $j = 1, 2, .., 1022$. Since our data is purely real we can fill in the remaining Fourier components, negative frequencies, with the complex conjugate of the corresponding positive frequencie components after they are selected from the distribution.

$$\widetilde{Z}'_{-k} = \widetilde{Z}'^{*}_{k} \tag{8}$$

The final synthetic MOSES row,

$$Z^{'} = \mathcal{F}_{y}^{-1}[\widetilde{Z}^{'}], \tag{9}$$

is 2048 elements long. After generating a large number of synthetic arrays we can compare their distribution of autocorrelation and power spectra to that of the MOSES image rows.

For the purposes of significance testing we generated 10,000 sets of three arrays, one array for each order.

2.5. Forward Model

Four EIT images selected as close to the viewing time as possible.
Peak Formation temperature of Chianti lines is used to select most fitting image.
We should consider whether using weighted combinations of these images was really the right thing to do. Possibly by comparing the results one way or another.

2.6. Fitting

Using a MCMC to thoroughly explore the parameter space and generate error bars on fit parameters. More work to be done here.

3. Results

Synthetic images of best fit. Quantify extra spectral content. Comment on extra He II emission unaccounted for by Chianti.

4. Discussions/Conclusions

Implications for future, design changes incorporated in ESIS (field stop, line selection, dispersion increase?). Possibly examine the spectra surrounding Ne VII 465 Å. Do we have the MOSES II throughput curves?

References

Fox, J.L., Kankelborg, C.C., Thomas, R.J.: 2010, A Transition Region Explosive Event Observed in He II with the MOSES Sounding Rocket. **??***jnlApJ* **719**, 1132. DOI. ADS. [Fox2010]

Rust, T.L.: 2017, Explosive Events in the Quiet Sun: Extreme Ultraviolet Imaging Spectroscopy Instrumentation and Observations. PhD thesis, Montana State University. ADS. [Rust2017]